Electronic Supplementary Material

Graphene oxide-decorated $Fe_2(MoO_4)_3$ microflowers as a promising anode for lithium and sodium storage

Chunhua Han[1] (✉), Xiaoji Ren[1], Qidong Li[1], Wen Luo[1,2], Lei Huang[1], Liang Zhou[1], and Liqiang Mai[1,†] (✉)

[1] *State Key Laboratory of Advanced Technology for Materials Synthesis and Processing, Wuhan University of Technology, Luoshi Road 122, Wuhan 430070, China*

[2] *Laboratoire de Chimie et Physique: Approche Multiéchelles des Milieux Complexes, Institut Jean Barriol, Université de Lorraine, 57070 Metz, France*

[†] *Present address: Department of Chemistry, University of California, Berkeley, California 94720, USA*

Supporting information to https://doi.org/10.1007/s12274-017-1742-9

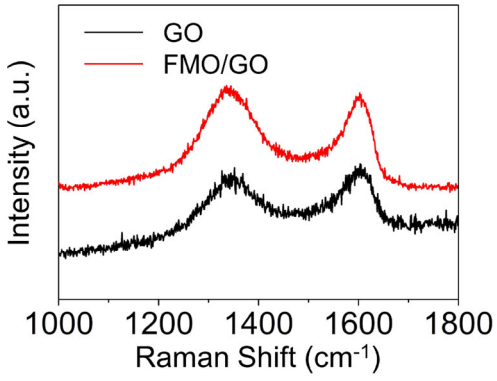

Figure S1 Raman spectra of FMO/GO, GO.

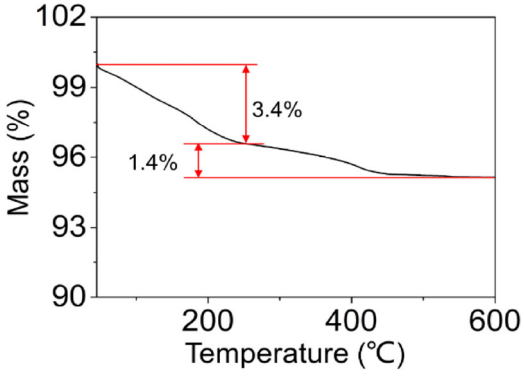

Figure S2 TG curve of FMO/GO.

Address correspondence to Liqiang Mai, mlq518@whut.edu.cn; Chunhua Han, hch5927@whut.edu.cn

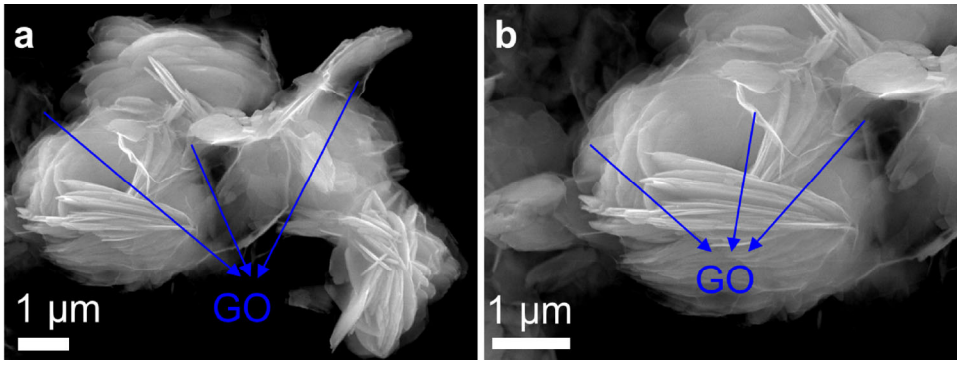

Figure S3 (a, b) SEM images of FMO/GO.

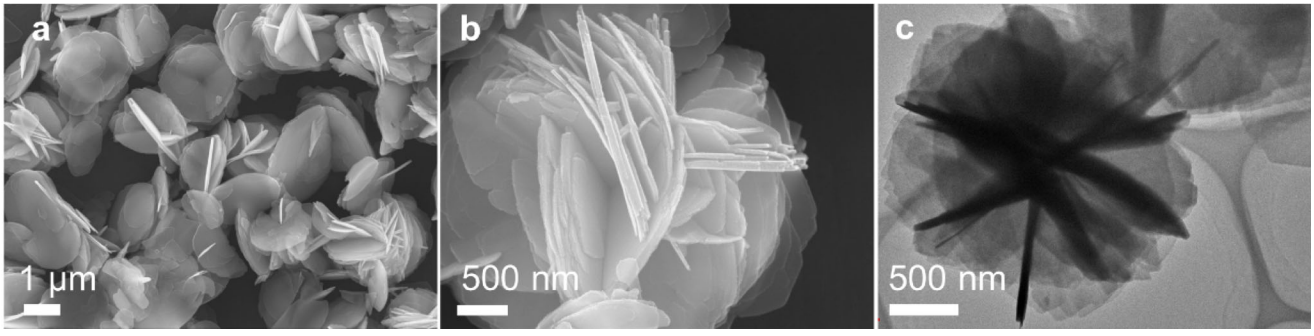

Figure S4 SEM (a and b) and TEM (c) images of FMO.

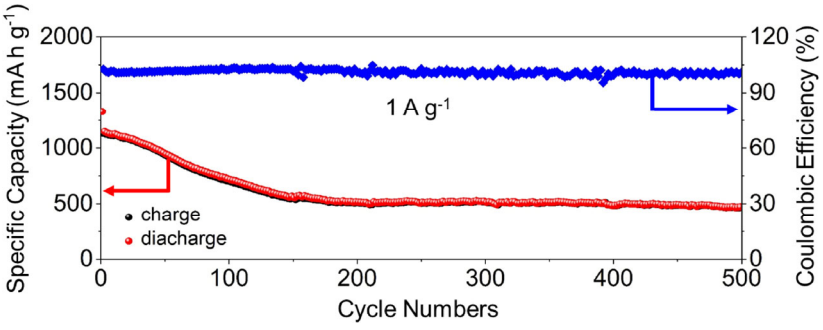

Figure S5 The long-term cycling performance of FMO/GO at 1 A g^{-1} in LIBs.

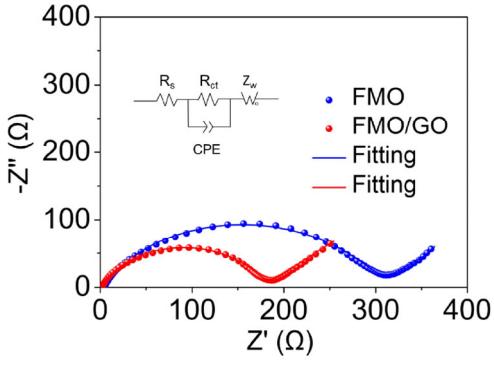

Figure S6 Nyquist plots of FMO and FMO/GO in lithium storage.

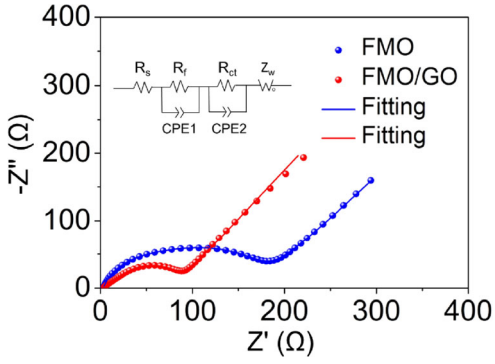

Figure S7 Nyquist plots of FMO and FMO/GO in sodium storage.

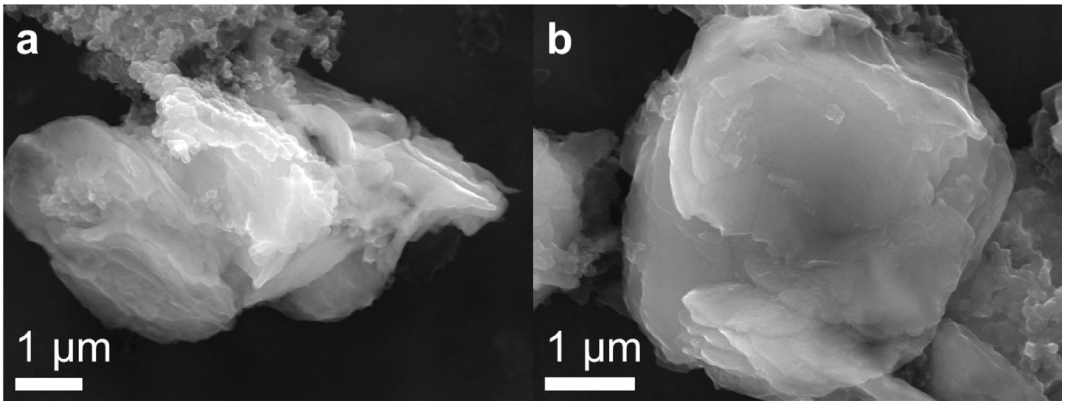

Figure S8 SEM images of (a) FMO and (b) FMO/GO after 50 cycles in sodium storage.

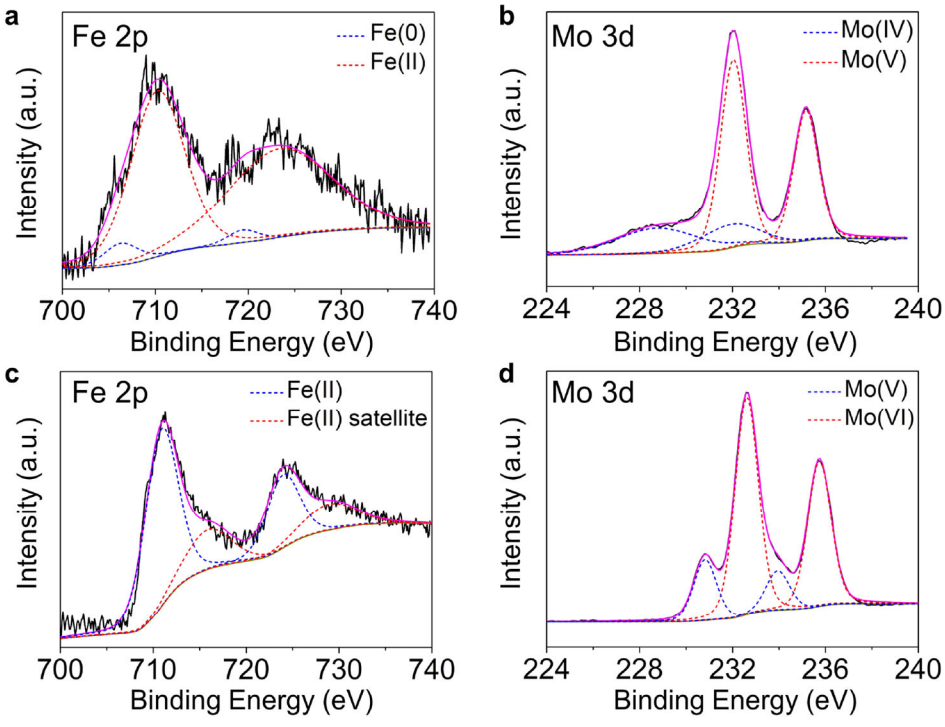

Figure S9 XPS spectra of FMO when discharged to 0.01 V (a, b) and charged to 3 V (c, d).

Table S1 Comparison of the results in this study with reported performance of transition metal molydbates in lithium storage.

Sample	Rate capability	Cycling stability	Reference
$Fe_2(MoO_4)_3$/MCNCT	600 mA h g^{-1} at 1200 mA g^{-1}	1033 mA h g^{-1} at 120 mA g^{-1} (200 cycles)	S1
$Fe_2Mo_3O_8$-RGO		574 mA h g^{-1} at 3000 mA g^{-1} (40 cycles)	S2
$FeMoO_4$ nanocubes	215 mA h g^{-1} at 2000 mA g^{-1}	926 mA h g^{-1} at 100 mA g^{-1} (80 cycles)	S3
$CoMoO_4$ NP/RGO	600 mA h g^{-1} at 740 mA g^{-1}	600 mA h g^{-1} at 740 mA g^{-1} (600 cycles)	S4
$MnMoO_4$@C	362 mA h g^{-1} at 5000 mA g^{-1}	1000 mA h g^{-1} at 100 mA g^{-1} (200 cycles)	S5
$NiMoO_4$	600 mA h g^{-1} at 3200 mA g^{-1}	1028 mA h g^{-1} at 200 mA g^{-1} (120 cycles)	S6
Carbon-coated nanophase $CaMoO_4$		508 mA h g^{-1} at 60 mA g^{-1} (20 cycles)	S7
$Mn_2Mo_3O_8$-graphene	671 mA h g^{-1} at 1500 mA g^{-1}	950 mA h g^{-1} at 200 mA g^{-1} (40 cycles)	S8
FMO/GO	685 mA h g^{-1} at 10 A g^{-1}	1220 mA h g^{-1} at 200 mA g^{-1} (50 cycles)	our work

Table S2 Comparison of the results in this study with reported performance of transition metal molydbates in sodium storage.

Sample	Rate capability	Cycling stability	Reference
$Ag_2Mo_2O_7$	100 mA h g^{-1} at 500 mA g^{-1}	190 mA h g^{-1} at 20 mA g^{-1} (70 cycles)	S9
$Na_{0.3}MoO_2$	65 mA h g^{-1} at 500 mA g^{-1}	124 mA h g^{-1} at 20 mA g^{-1} (50 cycles)	S10
$Bi_2(MoO_4)_3$/C	100 mA h g^{-1} at 3000 mA g^{-1}	320 mA h g^{-1} at 150 mA g^{-1} (100 cycles)	S11
FMO/GO	107 mA h g^{-1} at 10 A g^{-1}	307 mA h g^{-1} at 100 mA g^{-1} (100 cycles)	our work

References

[S1] Pramanik, A.; Maiti, S.; Mahanty, S. Superior lithium storage properties of $Fe_2(MoO_4)_3$/MWCNT composite with a nanoparticle (0D)-nanorod (1D) hetero-dimensional morphology. *Chem. Eng. J.* **2016**, *307*, 239–248.

[S2] Sun, Y. M.; Hu, X. L.; Luo, W.; Shu, J.; Huang, Y. H. Self-assembly of hybrid $Fe_2Mo_3O_8$–reduced graphene oxide nanosheets with enhanced lithium storage properties. *J. Mater. Chem. A* **2013**, *1*, 4468–4474.

[S3] Ju, Z. C.; Zhang, E.; Zhao, Y. L.; Xing, Z.; Zhuang, Q. C.; Qiang, Y. H.; Qian, Y. T. One-pot hydrothermal synthesis of $FeMoO_4$ nanocubes as an anode material for lithium-ion batteries with excellent electrochemical performance. *Small* **2015**, *11*, 4753–4761.

[S4] Yao, J. Y.; Gong, Y. J.; Yang, S. B.; Xiao, P.; Zhang, Y. H.; Keyshar, K.; Ye, G. L.; Ozden, S.; Vajtai, R.; Ajayan, P. M. $CoMoO_4$ nanoparticles anchored on reduced graphene oxide nanocomposites as anodes for long-life lithium-ion batteries. *ACS Appl. Mater. Interfaces* **2014**, *6*, 20414–20422.

[S5] Guan, B. Q.; Sun, W. W.; Wang, Y. Carbon-coated $MnMoO_4$ nanorod for high-performance lithium-ion batteries. *Electrochim. Acta* **2016**, *190*, 354–359.

[S6] Wang, B.; Li, S. M.; Wu, X. Y.; Tian, W. M.; Liu, J. H.; Yu, M. Integration of network-like porous $NiMoO_4$ nanoarchitectures assembled with ultrathin mesoporous nanosheets on three-dimensional graphene foam for highly reversible lithium storage. *J. Mater. Chem. A* **2015**, *3*, 13691–13698.

[S7] Sharma, N.; Shaju, K. M.; Rao, G. V. S.; Chowdari, B. V. R.; Dong, Z. L.; White, T. J. Carbon-coated nanophase $CaMoO_4$ as anode material for Li ion batteries. *Chem. Mater.* **2004**, *16*, 504–512.

[S8] Sun, Y. M.; Hu, X. L.; Luo, W.; Huang, Y. H. Hierarchical self-assembly of $Mn_2Mo_3O_8$–graphene nanostructures and their enhanced lithium-storage properties. *J. Mater. Chem.* **2011**, *21*, 17229–17235.

[S9] Chen, N.; Gao, Y.; Zhang, M. N.; Meng, X.; Wang, C. Z.; Wei, Y. J.; Du, F.; Chen, G. Electrochemical properties and sodium-storage mechanism of $Ag_2Mo_2O_7$ as the anode material for sodium-ion batteries. *Chem.–Eur. J.* **2016**, *22*, 7248–7254.

[S10] Zhu, K.; Guo, S. H.; Yi, J.; Bai, S. Y.; Wei, Y. J.; Chen, G.; Zhou, H. S. A new layered sodium molybdenum oxide anode for full intercalation-type sodium-ion batteries. *J. Mater. Chem. A* **2015**, *3*, 22012–22016.

[S11] Sottmann, J.; Herrmann, M.; Vajeeston, P.; Ruud, A.; Drathen, C.; Emerich, H.; Wragg, D. S.; Fjellvåg, H. Bismuth vanadate and molybdate: Stable alloying anodes for sodium-ion batteries. *Chem. Mater.* **2017**, *29*, 2803–2810.